# Design of Ultra-wideband and Transparent Absorber based on Resistive Films

**Xinru Lu [1], Juan Chen [2], Youqi Huang [3], Zixian Wu [1], and Anxue Zhang [1]**

[1] School of Electronic and Information Engineering
Xi'an Jiaotong University, Xi'an, 710000, China

[2] The Shenzhen Research School
Xi'an Jiaotong University, Shenzhen, 518000, China
chen.juan.0201@mail.xjtu.edu.cn

[3] China Building Materials Academy Co., Ltd
China Building Materials Academy Co., Ltd, Beijing, 100024, China

***Abstract*** ─ Researching and developing of ultra-wideband capability and high light transmittance have been hot issues in the field of new artificial electromagnetic stealth material. In this paper, a novel transparent metamaterial absorber, made of resistive films and glass, has been presented. The simulation results show that, under the incidence of plane wave, the absorber realizes high absorption during frequency range from 3.5 GHz to 18.5 GHz while keeping insensitive to polarization. A prototype has been fabricated and tested, and the measurement results are in good consistent with simulation. Along with its high transmittance and superior absorption, we expect that the absorber has great potential applications in RCS (Radar Cross Section) reduction and electromagnetic shielding.

***Index Terms*** ─ Absorber, broadband, RCS reduction, resistive film, transparent.

## I. INTRODUCTION

Meta-material absorber, belonging to the category of artificial electromagnetic materials, has attracted much attention since Landy et al. [1] first proposed the "PMA" (perfect meta-material absorber) which achieved more than 88% absorption at 11.5 GHz in 2008. Changes of meta-material structure could affect its electrical parameters: effective permeability ($\mu_{eff}$) and permittivity ($\varepsilon_{eff}$), in this way the impedance of meta-material is altered dependently. In transmission line theory, when the impedance of meta-material reaches to 377 Ω, meta-material realizes perfect impedance matching with free space. So, if an electromagnetic wave is incident on the meta-material, there would be no reflected energy. Especially when the meta-material contains metal backplane, the energy of incident wave is completely absorbed in it as there is no reflected or transmitted wave. Meta-material absorber offers a number of prominent technical advantages including thin thickness, lightweight, and strong flexibility, which surpasses traditional absorbing materials. With these advantages, meta-material absorber has immense potential in electromagnetic application, such as stealth, shielding, and electromagnetic compatibility (EMC) [2]. So far, researches on meta-material absorber have been reported. Great efforts have been devoted to improve the ability to work in wider domain of frequency, for example, in 3~20 GHz. This is because the regime from 3 GHz to 20 GHz covers most of communication bands for military radar. However, narrow bandwidth of absorption has always been the key difficulty in design [3].

In order to resolve the problem of narrow absorbing band, various methods including employing multi-resonant [4], [5], multi-layered structures [6] and new materials [7-10], have been brought up. Nevertheless, these absorbers have drawbacks of large thickness, limited bandwidth, and difficult fabrication. Apart from that, absorber loaded with resistance, causing circuit resonance, has obtained better result for broadening bandwidth.

In addition, traditional absorbing materials are often composed of magnetic metal powders, carbon materials and ferrite [11], and use metal plates as backplane in general. Their common feature is non-transparent, which means they cannot be used to in these situations which both need wave absorption and transparency, such as the display screen and window.

In this paper, we present a transparent, ultra-wideband and polarized-independent absorber. As the absorption is based on resistive loss from circuit resonance in structure, the working bandwidth is greatly broadened. The absorber is made of indium tin oxide (ITO) [12], polyvinyl butyral (PVB), and glass, so it has high optical transparency. It can achieve more than 70% absorption in the frequency range from 3.5 GHz to 18.5 GHz, and

*Submitted On: December 3, 2018*
*Accepted On: March 3, 2019*

the bandwidth is 136.3% of the central frequency. As shown in Table 1, this absorber exhibits larger bandwidth in contrast to recent papers on transparent and broadband meta-material absorber. Although some absorbers have higher absorptions, their bandwidth is not satisfied. A sample with 10×20 cells is fabricated and tested. The measured results show good agreements with simulation results.

## II. DESIGN AND SIMULATION

In the field of meta-material absorber, it is most common, by using electromagnetic resonance, to actualize energy consumption in structure. When waves are incident on the surface, electrical resonance happens within the metal structure of each cell, and magnetic resonance happens between adjacent cells [16]. Energy vibrates intensively between dielectric and metal at resonant frequencies, and finally it is absorbed in dielectric because of dielectric loss. However, as electromagnetic resonance occurs merely at several frequency points, the absorption bandwidth is usually narrow. When resistance elements such as resistive film are introduced in the structure, circuit resonance which is more stable for frequency changes [17], occurs in RLC circuit formed by resistive film, dielectric medium, and metal backplane. Good impedance matching is achieved by proposed structure in wide frequency range, hence, the absorption bandwidth can be broadened significantly.

The schematic of the absorber structure is shown in Fig. 1. The absorber is composed of five layers (glass, resistive film, PVB, glass and resistive film, from top to bottom). The pattern of resistive film that is located in middle layer is given in Fig. 1 (c). We choose resistive film with low surface resistance as backplane to avoid transmitted wave. Both glass and PVB are lossless, and their relative permittivity are 6.2 and 3.1, respectively. The entire thickness of absorber is 5.38 mm, which is only 0.074 $\lambda$ with regard to the lowest working frequency 3.5 GHz. $R_{S1}$ and $R_{s2}$ represent the resistances of resistive films located in the middle and bottom of structure, respectively. Related parameters are given below: $R_{S1}$= $R_{s2}$=20 Ohm/square, h1=3 mm, h2=0.38 mm, h3=2 mm, P=10.5 mm, L=9.5 mm, w=5 mm. Figure 2 shows a finite surface, which is obtained from arranging cells of absorber periodically along x-axis and y-axis. When electromagnetic waves are incident on the surface along –z axis direction, the large amount of wave energy is absorbed in the structure, leaving little reflected and transmitted energy.

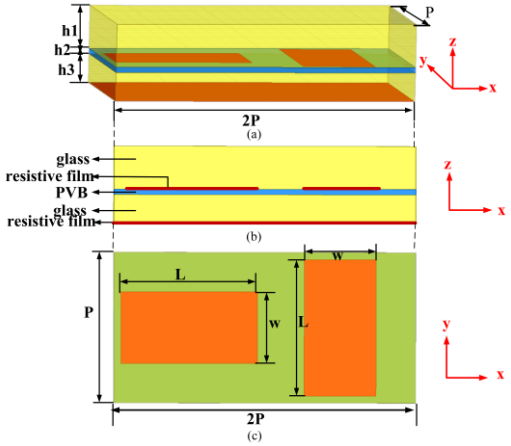


Fig. 1. Schematic of the absorber including: (a) structure of one unit cell, (b) sectional view, and (c) the pattern of resistive film.

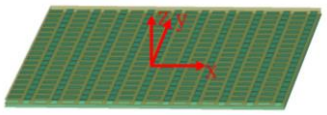

Fig. 2. A finite surface of absorber which is obtained from periodic arrangement of cells.

In order to give an accurate explanation to the mechanism of absorption, equivalent circuit model is presented according to the structure of absorber, shown in Fig. 3. $Z_0$, $Z_1$, and $Z_2$ are the impedances of free space, glass, and PVB material, where $Z_0 = 377\ \Omega$, $Z_1 = Z_0/\sqrt{\varepsilon_r(glass)}$, $Z_2 = Z_0/\sqrt{\varepsilon_r(PVB)}$. The impedance of the lossy FSS can be represented though a serial circuit formed by $R_1$, $L_1$ and $C_1$. $R_1 \approx R_{S1} \cdot D/A$ [18], where $D = 2 \cdot P^2$, $A = 2 \cdot w \cdot L$. $R_2 = R_{S2}$, which represents the impedance of resistive sheet. The lengths of equivalent transmission lines are also given in Fig. 3, corresponding to the thickness of dielectrics. Therefore, Zin is formed by series and parallel RLC resonance circuit and dependent on design parameters of structure. Ideally, when resonance happens, it makes $Z_{in}$ equal to $Z_0$ and there are no reflected waves. Adjusting parameter of structure to generate multi-resonant frequency helps to form an ultra-wide absorption band.

Table1: Comparisons of proposed and some other absorbers

| Ref. | Absorbing Ability | Principle | Transparency |
|---|---|---|---|
| [13] | More than 70% in 12.5 ~ 17G | Based on resistive films | Yes |
| [14] | More than 90% in 8.5 ~ 11G and 14.5 ~ 16.5G | Based on resistive films | Yes |
| [15] | More than 90% in 5.8 ~ 12.2G | Based on resistive films | Yes |
| This paper | More than 70% in 3.5 ~ 18.5G | Based on resistive films | Yes |

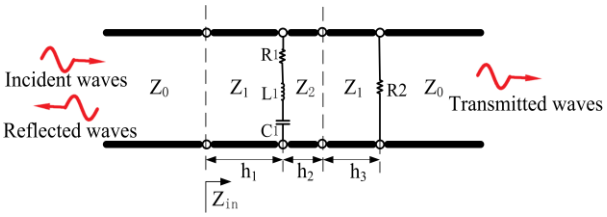


Fig. 3. Equivalent circuit model according to the structure of absorber.

Reflection (S11) and transmission (S21) coefficients from simulation are showed in Fig. 4. From Fig. 4 (a), it can be seen that S11 is lower than -5 dB in the region 3.5~18.5 GHz, which means the absorber can realize the function of stealth during an ultra-wide range of frequency band. From Fig. 4 (b), S21 is less than -15 dB in 1~21 GHz. It means the absorber has the ability of electromagnetic shielding, as the energy of transmission wave is weak enough to be ignored.

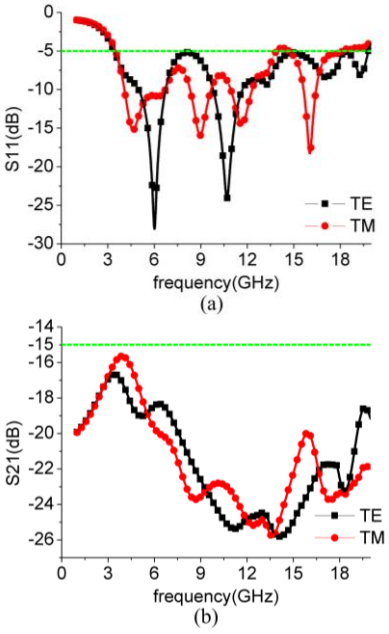


Fig. 4. (a) Reflection coefficients and (b) transmission coefficients from simulation, under the normal incidences of TE (transverse electric) and TM (transverse magnetic) waves.

The property of absorber can be quantitatively analyzed by the absorption rate. The absorption rate is calculated as follows:

$$A(\omega) = 1 - |S_{11}|^2 - |S_{21}|^2. \quad (1)$$

The calculated result of absorption rate is shown in Fig. 5. It can be seen from this figure that the absorption rate is more than 70% in the frequency range from 3.5 GHz to 18.5 GHz. Insensitivity is demonstrated in Fig. 5 simultaneously, since absorptions for TE and TM waves are roughly similar. Through simulation results, it proves that the absorber has ultra-wideband and insensitive absorption in band 3.5~18.5 GHz.

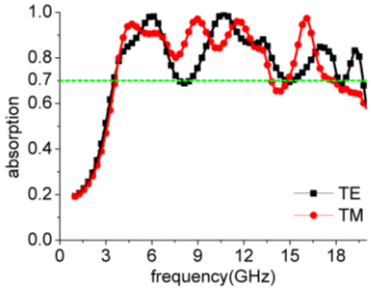


Fig. 5. Absorption rate from calculation, under the normal incidences of TE and TM waves.

In this section, we will analyze the effect of the parameters of $R_{S1}$, $R_{s2}$ and h1 on the absorption rate. We only vary one parameter in the study while keeping others unchanged.

The influence of $R_{S1}$ is investigated, as shown in Fig. 6 (a). When $R_{S1}$ increases from 20 Ω to 140 Ω, two obvious resonate peaks, accompanying more efficient absorptions, appear at 6 GHz and 16.5 GHz. But the absorption rates in the transition band between these two peaks, are rapidly reduced. Taking into account the overall performance in 3~20 GHz, it is most suitable to set $R_{S1}$ as 20 Ω. It can be observed that the absorption rates around two resonant peaks are not deteriorated excessively and those during the transition band remain at a relatively high level.

Figure 6 (b) shows the variation of absorbing with respect to $R_{s2}$. As the resistance of bottom resistive film rises, the performances in 3~20 GHz are gradually better whereas those in 1~3 GHz tend to be opposite.

The variation of absorption rate with respect to h1 is depicted in Fig. 6 (c). When h1=0, absorption rates are divided into two absorption peaks around 8.25 GHz and 15GHz, and those in the transition band are low. After adding glass above the absorber and setting thickness of glass as 3 mm, the absorption is improved in general and achieves wide-band absorption efficiency. However, when h1 increases to 6mm, the absorptions in 3.25~12 GHz become deteriorated. Therefore, we choose 3mm as the proper thickness of upper glass. It can be found that, by adding glass with proper thickness above the structure, the impedance of absorber gets adjusted [19], causing better impedance matching with air and wider absorption efficiency. Compared with absorber without upper glass, in particular, this impedance adjusting solves the problem that it is difficult to realize high absorption in low frequency band.

As we mentioned before, perfect impedance matching between absorber and air occurs when relative impedance of absorber is close to 1. In order to validate the impedance matching between absorber and air, the relative impedance of absorber is quantitively calculated according to [20]:

$$z(\omega) = \sqrt{\frac{(1+S_{11})^2 - S_{21}^2}{(1-S_{11})^2 - S_{21}^2}}, \quad (2)$$

where S11 and S21 are from simulation results, under incidence of TE waves. Module value of $z(\omega)$ is then obtained and displayed in Fig. 7. Module value of relative impedance mainly appears around 0.6 in 3.5~18.5 GHz. It is also observed from Fig. 7 and Fig. 5, when the module value of $z(\omega)$ is closer to 1, it helps improve the impedance matching; as a result, the absorber has better absorption efficiency.

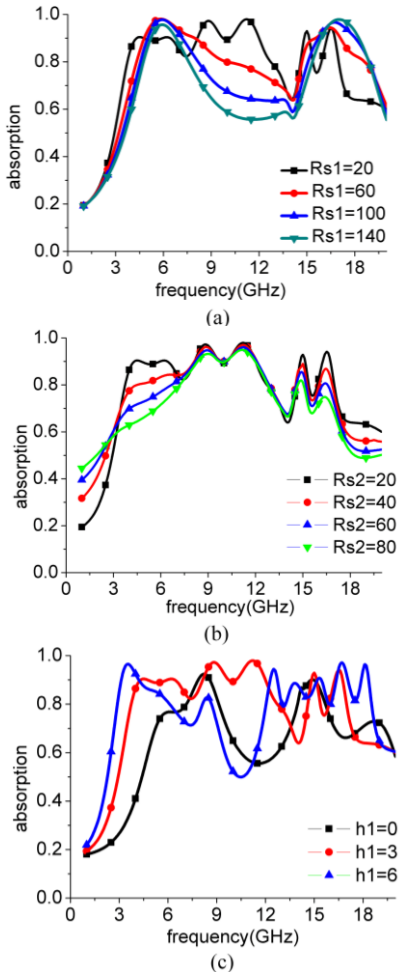


Fig. 6. Absorption rates when changing the values of parameters, and h1, shown in (a), (b), and (c), respectively.

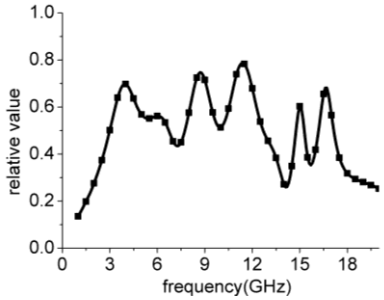


Fig. 7. Module value of relative impedance from calculation.

## III. FABRICATION AND MEASUREMENT

To experimentally demonstrate the efficiency of absorber, a sample of absorber obtained by the periodic arrangement of 10×20 cells, whose model structure is shown in Fig. 2, has been fabricated and tested. The ITO films with 20 Ohm/square are deposited on two plates of glass with different thickness by magnetron sputtering method. The pattern shown in Fig. 1 (c) is then etched on the ITO using laser etching technique. The sample is finally obtained by assembling two plates of glass with PVB. Prototype under weak and strong light is shown in Fig.8 (a) and Fig. 8 (b), respectively, which validates the transparency of the absorber.

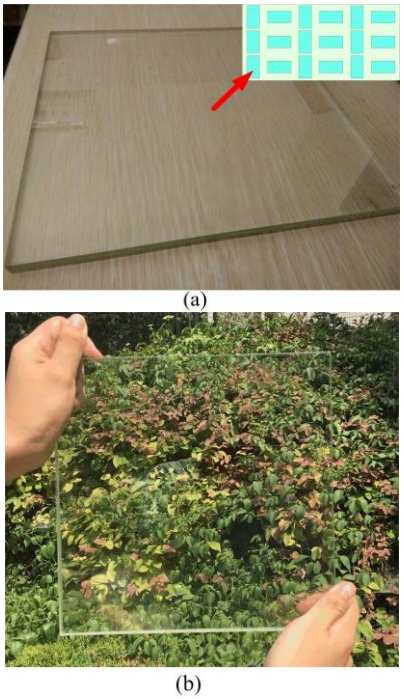


Fig. 8. (a) Photograph of sample under weak light, and (b) photograph of sample under strong light.

Figure 9 (a) shows the installation that measures the reflection coefficient of sample. Measurement is carried out in microwave anechoic chamber. Two horn antennas are placed at the ends of the revolving arms separately. One antenna serves as transmitter and the other is for reception. The sample is placed in the center of the revolving stage. The transmitter and receiver make up 20° towards the sample. The sample keeps enough distance with antennas to satisfy far-field condition. For testing of transmission coefficient, shown in Fig. 9 (b), transmitter is right in front of the sample, while receiver stands in the opposite.

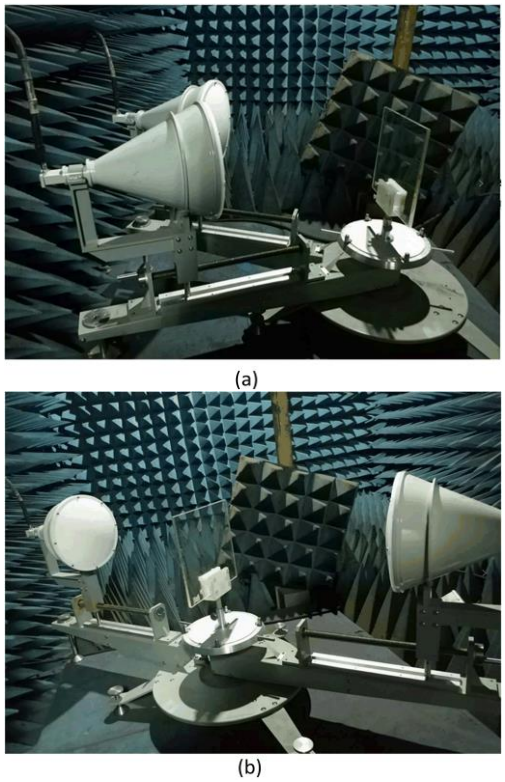


Fig. 9. (a) Photograph of experimental setup for reflection measurement, and (b) photograph of experimental setup for transmission measurement.

Measurement and simulation results are both shown in Fig. 10 to make a comparison. In this simulation, the absorber is 10×20 cells with same size as the sample, to reduce the effect of the size on the measured and simulated results. From Fig. 10, we can see that, under the incidence of plane wave, S11 from measurement achieves less than -5 dB in the range 3.5~18.5 GHz; S21 achieves less than -15dB during the whole working band. The measurement results are in good agreements with the simulation of finite absorber.

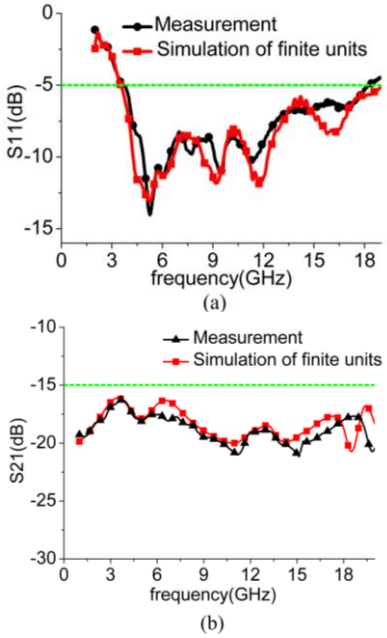


Fig. 10. The comparison between the measured result and simulated result: (a) for S11 and (b) for S21.

## IV. CONCLUSION

In this paper, an ultra-wideband and transparent absorber is presented. The absorber is made of ITO, PVB, and glass, so it has the property of high light transmission. Lossy circuit resonance happens in the absorber structure under the incidence of plane wave, which helps broaden the absorption bandwidth. The novelty of structure attributes to the upper glass of absorber which adjusts impedance matching between the absorber and air. The absorber, validated by experiment and simulation, has over 70% absorption rates in the band 3.5~18.5 GHz. Owing to its excellent performance, simple structure, and convenient realization, the absorber has great application potential in the field of transparent stealth and electromagnetic shielding.

## ACKNOWLEDGMENT

This work was supported by Technology Program of Shenzhen (Grant No. JCYJ20170816100722642), and also supported by the Natural Science Foundation of Guangdong Province (Grant No. 2018A030313429).

## REFERENCES

[1] N. I. Landy, S. Sajuyigbe, J. Mock, D. R. Smith, and W. J. Padilla, "Perfect metamaterial absorber," *Physical Rev. Lett.*, vol. 100, no. 20, p. 207402, 2008.

[2] L. Yuan, X. Shen, S. Cui, and L. Fan, "Progress

and prospect of transparent and electromagnetic shielding material," *NA Mater. Science and Eng*., vol. 30, no. 2, pp. 82-84, 2007.

[3] Y. Peng, V. B. Lucas, H. Yongjun, and W. Jiang, "Broadband metamaterial absorbers," *Adv. Opt. Mater*., p. 1800995, 2018.

[4] M. B. Ghandehari, N. Feiz, and H. Bolandpour, "Design a multiband perfect metamaterial absorber based on hexagonal shapes," *ACES Conference*, 2015.

[5] Y. Ozturk and A. E. Yilmaz, "Multiband and perfect absorber with circular fishnet metamaterial and its variations," *ACES Journal*, vol. 31, no. 12, 2016.

[6] D. Wen, H. Yang, Q. Ye, and M. Lin, "Broadband metamaterial absorber based on a multi-layer structure," *Phys. Scr*., vol. 88, p. 015402, 2016.

[7] J. Chen, J. Li, and Q. Liu, "Designing graphene-based absorber by using HIE-FDTD method," *IEEE T. Antenna Propag*., vol. 65, no. 4, pp. 1896-1902, 2017.

[8] J. Chen, J. Li, and Q. Liu, "Analyzing graphene-based absorber by using WCS-FDTD method," *IEEE T. Micorw. Theory*, vol. 65, no. 10, pp. 3689-3696, 2017.

[9] N. Xu, J. Chen, J. Wang, X. Qin, and J. Shi, "Dispersion HIE-FDTD method for simulating graphene-based absorber," *IET Microw. Antenna P*., vol. 11, no. 1, pp. 92-97, 2017.

[10] N. Xu, J. Chen, J. Wang, and X. Qin, "A dispersive WCS-FDTD method for simulating graphene-based absorber," *J. Electromag. Wave*, vol. 31, no. 18, pp. 2005-2015, 2017.

[11] V. M. Petrov and V. V. Gagulin, "Microwave absorbing materials," *Inorg. Mater*., vol. 37, no. 2, pp. 93-98, 2001.

[12] Y. Qiu, Y. Chen, C. Zu, and Y. Jin, "Research progress of ITO thin films," *Advanced Ceramics*, vol. 37, pp. 304-324, 2016.

[13] Y. Da, X. Wei, and Y. Xu, "Experimental demonstration of transparent microwave absorber based on graphene," *Proceedings of 2016 IEEE MTT-S International Wireless Symposium (IWS)*, Shanghai, China, Mar. 2016.

[14] B. Zhou, D. Wang, W. Jia, and Y. Zhao, "Design and properties of optically transparent and dual band microwave absorbing metamaterial," *J. of Microwaves*, vol. 32, pp. 46-50, 2016.

[15] T. Jang, H. Youn, Y. Shin, and L. J. Guo, "Transparent and flexible polarization-independent microwave broadband absorber," *ACS Photonics*, vol. 1, pp. 279-284, 2014.

[16] X. Huang, Q. Fu, and F. Zhang, "Research advances of metasurface," *Aero Weapon*, vol. 1, pp. 28-34, 2016.

[17] Z. Zhou, D. Huang, X. Liu, W. Mou, and F. Kang, "Application developments of metamaterial in wideband microwave absorbing materials," *Material Engineering*, vol. 5, pp. 91-96, 2014.

[18] F. Costa and A. Monorchio, "Analysis and design of ultra-thin electromagnetic absorbers comprising resistively loaded high impedance surfaces," *IEEE T. Antenna Propag*., vol. 58, 2010.

[19] Y. Shen, Z. Pei, and S. Qu, "Design and fabrication of a wideband frequency selective surface absorber loaded with a high dielectric thin layer," *Journal of Functional Material*, vol. 19, no. 46, pp. 19075-19079, 2015.

[20] D. Smith, D. Vier, T. Koschny, and C. M. Soukoulis, "Electromagnetic parameter retrieval from inhomogeneous metamaterials," *Phys. Rev. Lett*., vol. 71, p. 036617, 2005.